JOC The Journal of Organic Chemistry

Article

pubs.acs.org/joc

Oxygen-Initiated Chain Mechanism for Hydride Transfer Between NADH and NAD$^+$ Models. Reaction of 1-Benzyl-3-Cyanoquinolinium Ion with *N*-Methyl-9,10-Dihydroacridine in Acetonitrile

Weifang Hao and Vernon D. Parker*

Department of Chemistry and Biochemistry, Utah State University, Logan, Utah 84322, United States

Supporting Information

ABSTRACT: A reinvestigation of the formal hydride transfer reaction of 1-benzyl-3-cyanoquinolinium ion (BQCN$^+$) with *N*-methyl-9,10-dihydroacridine (MAH) in acetonitrile (AN) confirmed that the reaction takes place in more than one step and revealed a new mechanism that had not previously been considered. These facts are unequivocally established on the basis of conventional pseudo-first-order kinetics. It was observed that even residual oxygen under glovebox conditions initiates a chain process leading to the same products and under some conditions is accompanied by a large increase in the apparent rate constant for product formation with time. The efficiency of the latter process, when reactions are carried out in AN with rigorous attempts to remove air, is low but appears to be much more pronounced when MAH is the reactant in large excess. On the other hand, the intentional presence of air in AN ([air] = half-saturated) leads to a much greater proportion of the chain pathway, which is still favored by high concentrations of MAH. The latter observation suggests that a reaction intermediate reacts with oxygen to initiate the chain process in which MAH participates. Kinetic studies at short times show that there is no kinetic isotope effect on the initial step in the reaction, which is the same for the two competing processes. Our observation of the chain pathway of an NADH model compound under aerobic conditions is likely to be of importance in similar biological processes where air is always present.

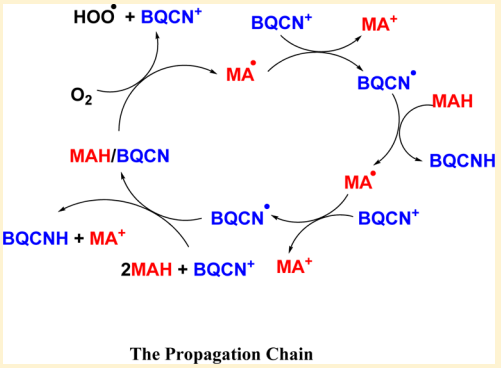

The Propagation Chain

INTRODUCTION

The *N*-methyl-9,10-dihydroacridine (MAH)/1-benzyl-3-cyanoquinolinium ion (BQCN$^+$) reaction in acetonitrile (AN) is of particular importance, since it has been studied extensively and is considered to be a genuine example of a direct one-step hydride transfer reaction, mainly due to the work of Kreevoy and co-workers.[1−6] The outer-sphere electron transfer (ET) mechanism can be considered to be unlikely due to the large standard potential difference (>1.2 V in AN) between that for the reduction of BQCN$^+$ and the oxidation of MAH.[7] A review,[8] as well as a number of recent studies[9−11] of the mechanisms for the reactions of various cations with NADH model compounds, illustrates that interest in these systems remains high.

In 2003, we proposed a three-step preassociation mechanism (Scheme 1) for the hydride transfer reaction between MAH and BQCN$^+$ in AN.[12] In 2008, Perrin[13] advanced the opinion that our data was not conclusive and on the basis of a nonkinetic ^{1}HNMR study suggested that the one-step mechanism is correct. Prior to 2008 we had found evidence[14−26] for similar complex behavior in a number of other organic reactions, and doubt was expressed[13] about our conclusions in these papers as well.

The present work is a part of our general effort to determine the mechanisms of fundamental organic reactions. In recent years, we have adopted methodology for mechanism analysis based solely upon whether or not the experimental data are consistent with the pseudo-first-order relationship, i.e., the linearity of $-\ln(1 - ER)$−time arrays, where ER is the extent of reaction. Application of this methodology has resulted in conclusive evidence that neither the formation of the 1,1-dimethoxy Meisenheimer complex derived from the reaction of 2,4,6-trinitroanisole with methoxide ion[27] nor the proton transfer reactions of simple nitroalkanes with hydroxide ion in water[28] take place by the mechanisms previously believed to be well-established.

In this paper, we show that the reaction of MAH with BQCN$^+$ in AN is further complicated by a multistep competing chain process under most circumstances. The chain process must be initiated by the reaction of oxygen with an intermediate, presumably a reactant complex, since the reaction of O_2 with MAH is very slow, but it is efficient even in the presence of residual oxygen under glovebox conditions as long as BQCN$^+$ is present in the AN solution. We also attempt to clarify the mechanism at short times, where the interference from the chain process is minimized.

Received: August 30, 2012
Published: October 1, 2012

 © 2012 American Chemical Society dx.doi.org/10.1021/jo301874q | J. Org. Chem. 2012, 77, 9286−9297

Scheme 1. Proposed Three-Step Mechanism for the Reaction of MAH with $BQCN^+$ in AN[a]

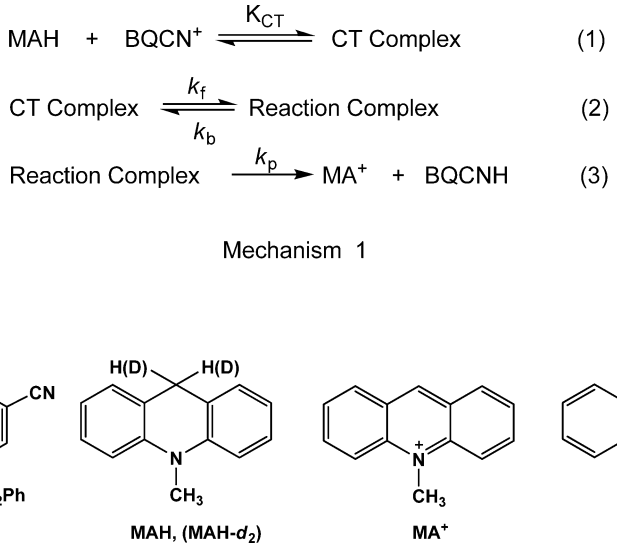

[a]This mechanism was proposed in 2003.[12]

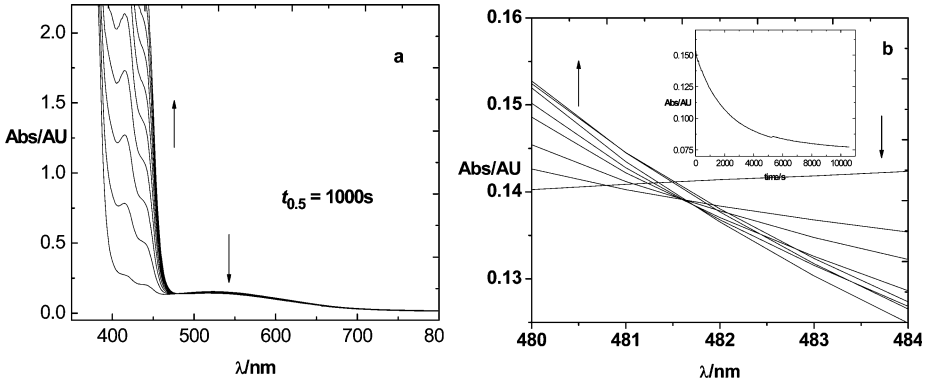

Figure 1. UV−vis absorption spectra for the reaction of $BQCN^+$ (0.04 M) with MAH (0.01 M) in AN at 298 K. (a) Half-life is 1000 s. (b) Time between spectra equals 25 min. (Inset) Absorbance−time decay curve recorded at 525 nm under the same conditions.

Table 1. Changes in the Apparent Pseudo-First-Order Rate Constants (k_{app}) as a Function of the Degree of Reaction Analyzed for the Reactions of MAH with $BQCN^+$ in AN at 298 K under Various Conditions at 430 nm

	$[BQCN^+]^a$		$[BQCN^+]$/air[b]		[MAH][c]		[MAH]/air[d]	
no. of half-lives analyzed	$10^4 \times k_{app}/s^{-1}$	$10^3 \times$ intercept	$10^4 \times k_{app}/s^{-1}$	$10^3 \times$ intercept	$10^4 \times k_{app}/s^{-1}$	$10^3 \times$ intercept	$10^4 \times k_{app}/s^{-1}$	$10^3 \times$ intercept
0.5	8.27	−2.30	11.8	−6.58	6.64	−0.284	6.22	1.82
1.0	8.58	−8.17	13.2	−24.4	6.64	−0.496	6.19	2.26
2.0	9.04	−26.2	15.3	−73.7	6.73	−5.64	6.32	−5.29
3.0	9.45	−52.0	17.3	−144	6.91	−20.6	6.59	−29.9
4.0	9.81	−82.5	19.2	−227	7.16	−49.5	6.94	−71.4

[a]$[BQCN^+]$ = 0.5 mM, [MAH] = 40 mM in AN containing only residual oxygen. [b]$[BQCN^+]$ = 0.5 mM, [MAH] = 40 mM in AN half-saturated with air. [c]$[BQCN^+]$ = 40 mM, [MAH] = 0.5 mM in AN containing only residual oxygen. [d]$[BQCN^+]$ = 40 mM, [MAH] = 0.5 mM in AN half-saturated with air.

RESULTS

Our previous work[12] on this reaction was carried out using a conventional UV−vis spectrophotometer and the kinetic conclusions were based on data recorded in the ER−time range from 0.05 to 0.5. The reason for this restriction was that we considered that the data at ER < 0.05 was uncertain due to the fact that manual mixing of the reactants was used. Under these conditions, we found that, at reaction temperatures below 308 K, we *could not* observe any deviations from simple first-order kinetics. Since that time our non-steady-state kinetic methods have continually developed and been improved significantly.[27−29] Due to the negative critique of our mechanism[13] and the incomplete nature of our experimental study,[12] the data that this paper is based on were obtained using our most recently developed kinetic techniques.[27−29]

The spectra illustrated in Figure 1 were obtained during the reaction of $BQCN^+$ (0.04 M) with MAH (0.01 M) in AN at 298 K. The absorbance due to the product MA^+ is indicated by the upward arrow in Figure 1a. The peak with maximum

dx.doi.org/10.1021/jo301874q | J. Org. Chem. 2012, 77, 9286−9297

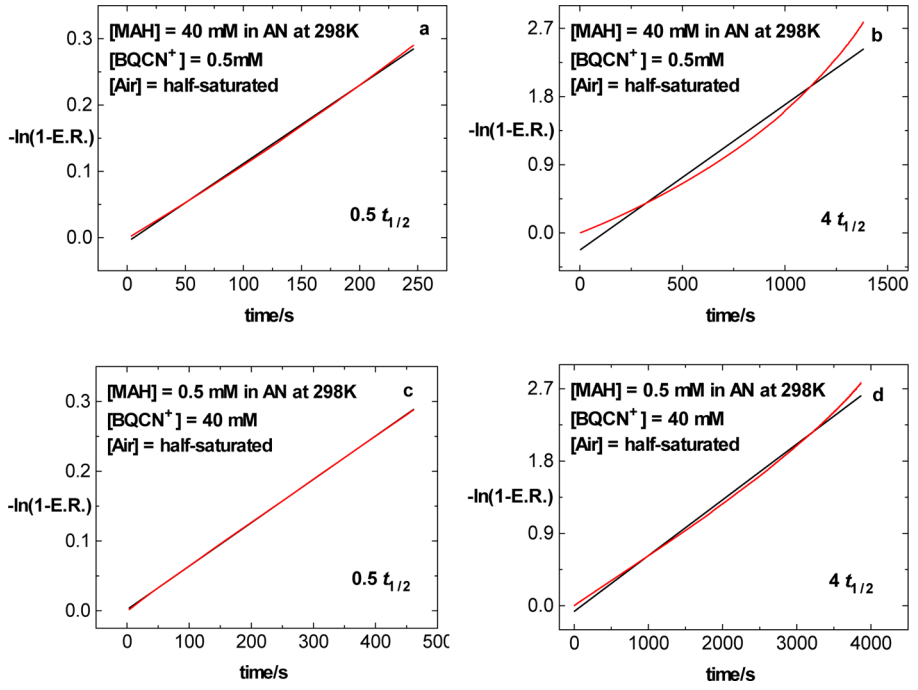

Figure 2. Pseudo-first-order plots for the reactions of $BQCN^+$ (0.50 mM) with MAH (40 mM) (a and b) and $BQCN^+$ (40 mM) with MAH (0.5 mM) (c and d) in AN half-saturated with air at 298 K at 430 nm.

absorbance at 525 nm, observed immediately after mixing, was observed to decay with time and disappear as the reaction approached completion, as shown in Figure 1b (insert). A close examination of the wavelength region around 481−482 nm revealed that several of the spectra intersect at about 481.6 nm but others do not, indicating that there is no true isosbestic point in that wavelength region. The species giving rise to the broad absorbance band at 525 nm is a charge-transfer complex. Similar spectra have been reported for MAH and related donors with a number of quinones as acceptor molecules.[30]

The answer to the question of whether or not the reaction of $BQCN^+$ with MAH in AN follows a one-step mechanism, even at temperatures below 308 K, can readily be obtained using a modification of the conventional −ln(1 − ER)−time profiles. All of kinetic work here is based upon the conversion of absorbance−time profiles to −ln(1 − ER)−time profiles for the evolution of MA^+.

Thus, whether or not the reactions conform to simple mechanism kinetics will be assessed by the fit of the least-squares correlation lines to the experimental data. In addition to the visual inspection of pseudo-first-order plots, the latter is readily accomplished by the quantitative comparison of slopes and intercepts as a function of the interval in the data analyzed with the expected result for a one-step mechanism. The latter is demonstrated by the data in Table 1.

The data in Table 1 allow for a close examination of deviations from pseudo-first-order behavior of the reactions of $BQCN^+$ with MAH in AN at 298 K and 430 nm. The data in column 2 show the k_{app} values for the reaction of excess MAH (40 mM) with $BQCN^+$ (0.5 mM) in AN under an attempt to exclude air. The k_{app} measured over the first 0.5 half-lives (HL) was observed to be equal to 0.000 827 s^{-1} and to vary uniformly to 0.000 981 s^{-1} as the data segment was increased to 4.0 HL. The intercepts of the corresponding first-order plots varied uniformly over a range of 36, as shown in column 3. Under comparable conditions, except that the reaction solution was half-saturated with air, a similar pattern of k_{app} as a function of the degree of reaction encompassed in the analysis was observed, but in this case (column 4), the variations were greater, 0.001 18−0.001 92 s^{-1}, and the corresponding intercepts (column 5) varied over a range of 34 over the same set of degree of reactions. A very similar trend was observed for the case (columns 6 and 7) when $BQCN^+$ was the excess reagent (40 mM) reacting with MAH (0.5 mM), in AN under conditions where rigorous attempts were made to exclude air. In this case, k_{app} varied between 0.000 664 and 0.000 716 s^{-1} in the same range as the other analyses. The values of k_{app} (column 8) changed from 0.000 622 s^{-1} at 0.5 HL to 0.000 694 s^{-1} at 4.0 HL with a large change in the intercept (column 9) when the reaction solution was half-saturated with air and $BQCN^+$ was the excess reagent (40 mM).

A more detailed procedure used is to divide the data arrays into 24 data segments on which the analysis is carried out. The times recorded for the data segments correspond to the center point of the segment. This procedure has been described in detail.[27] The successive series of rate constants (k_{app}) obtained can then be plotted vs the times at the midpoints of each segment. This procedure gives a clear indication of any changes in the values of the apparent pseudo-first-order rate constant (k_{app}) as the reaction proceeds. An advantage of the procedure is that standard deviations (SD) in data from multiple absorbance−time profiles are provided. The results obtained by this method are illustrated in the following sections for reactions carried out under the same four sets of conditions as illustrated in Table 1.

Conventional Pseudo-First-Order Analysis of the Reactions of MAH and $BQCN^+$ in Which either Reactant Acts as the Limiting or the Excess Reagent. The pseudo-first-order analyses of the reactions in which either $BQCN^+$ or MAH is the excess reactant are shown in the Supporting Information (Figure S-1). The comparison of the effect of which reactant is the excess reagent is illustrated by the pseudo-

dx.doi.org/10.1021/jo301874q | J. Org. Chem. 2012, 77, 9286−9297

Table 2. Changes in k_{app} and Standard Deviations (SD) as a Function of the Degree of Reaction Analyzed for the Reactions of MAH/MAH-d_2 (40 mM) with $BQCN^+$ (0.5 mM) in AN at 298 K in the Presence of Residual Oxygen at 430 nm

	MAH[a]								
	data set 1		data set 2		MAH-d_2[a]				
time	$10^4 \times k_{app}/s^{-1}$	$10^4 \times$ SD	$10^4 \times k_{app}/s^{-1}$	$10^4 \times$ SD	$10^4 \times k_{app}/s^{-1}$	$10^4 \times$ SD	$KIE_{app}(1)$	$KIE_{app}(2)$	segment
2.47	7.10	0.18	8.42	0.34	2.14	0.41	3.32	3.93	1
4.72	6.95	0.23	8.77	0.26	1.80	0.28	3.86	4.87	2
6.97	6.87	0.10	8.80	0.11	1.68	0.28	4.09	5.24	3
9.22	6.83	0.07	8.87	0.10	1.59	0.23	4.30	5.58	4
11.47	6.88	0.08	8.85	0.08	1.54	0.13	4.47	5.75	5
22.72	6.88	0.07	8.80	0.05	1.35	0.12	5.10	6.52	6
45.22	6.86	0.07	8.84	0.03	1.32	0.04	5.20	6.70	7
67.72	6.87	0.07	8.93	0.03	1.30	0.01	5.28	6.87	8
90.22	6.87	0.08	9.00	0.03	1.29	0.01	5.33	6.98	9
112.7	6.88	0.09	9.07	0.04	1.28	0.01	5.38	7.09	10
135.2	6.89	0.11	9.12	0.04	1.28	0.01	5.38	7.13	11
157.7	6.89	0.13	9.18	0.04	1.28	0.01	5.38	7.17	12
180.2	6.91	0.14	9.24	0.04	1.28	0.01	5.40	7.22	13
202.7	6.93	0.16	9.29	0.04	1.28	0.01	5.41	7.26	14
225.2	6.96	0.17	9.34	0.04	1.28	0.01	5.44	7.30	15
247.7	7.02	0.18	9.39	0.04	1.28	0.01	5.48	7.34	16
270.2	7.09	0.18	9.44	0.05	1.28	0.01	5.54	7.38	17
292.7	7.16	0.18	9.50	0.05	1.28	0.01	5.59	7.42	18
315.2	7.24	0.18	9.56	0.05	1.28	0.01	5.66	7.47	19
337.7	7.33	0.18	9.63	0.05	1.28	0.01	5.73	7.52	20
360.2	7.42	0.17	9.69	0.06	1.28	0.01	5.80	7.57	21
382.7	7.52	0.17	9.75	0.06	1.28	0.01	5.88	7.62	22
405.2	7.62	0.17	9.82	0.07	1.28	0.01	5.95	7.67	23
427.7	7.72	0.16	9.89	0.08	1.28	0.01	6.03	7.73	24

[a]Average of 10 stopped-flow repetitions.

first-order plots in which figures on the left (Supporting Information, Figure S-1a–c) are for the reaction in which [MAH] is in excess and those on the right (Supporting Information, Figure S-1a′–c′) are when [$BQCN^+$] is in excess. It will become obvious later that the reactant in excess has the greatest influence on the data. The reactions were followed by monitoring the evolution of product at 430 nm.

The most obvious result of a visual comparison of the pseudo-first-order plots on the left and the right of Figure S-1 (Supporting Information) is that deviations from the experimental data from the least-squares correlation lines are significantly greater when [MAH] is in excess than when [$BQCN^+$] is the excess reactant. A close examination of the plots reveals that there are deviations in all cases but that in the case of the plots constructed for data over less than 1 half-life, the deviations appear to be so small that it might be considered to be "justifiable" to attribute them to experimental error.

The effect of the presence of oxygen from air dissolved (half-saturated) in AN on the kinetic plots is illustrated in Figure 2 for the reactions of $BQCN^+$ (0.5 mM) with MAH (40 mM) and $BQCN^+$ (40 mM) with MAH (0.5 mM) over either 0.5 HL (Figure 2a,c) or 4 HL (Figure 2b,d). Acetonitrile half-saturated with air was used for a practical reason, i.e. the $BQCN^+$ solution saturated with air was mixed with the MAH solution that was protected from air in order to ensure that no reaction with oxygen takes place before mixing. The [O_2] in the half-saturated solution was estimated to be equal to 0.85 mM from the solubility of O_2 in AN reported.[31] The deviations of the correlation line from experimental data are obvious very early in the reaction in Figure 2a and is extreme when the correlation was carried out over 4 HL (Figure 2b), when [MAH] is in large excess. When $BQCN^+$ is the reactant in excess, deviation from the correlation is barely visible during the first HL (Figure 2c) and not nearly so severe at 4 HL (Figure 2d) as was observed in the previous case.

Reactions in the Presence of Residual Air. Successive Correlation Analysis of the Reactions of $BQCN^+$ with MAH/MAH-d_2 in AN at 298 K. The application of the successive correlation method (24-point procedure) to data obtained under the four different sets of reactant concentrations is illustrated in Tables 2, 3, 5, and 6 for data gathered over 1 HL while monitoring product formation in the range from 430 to 450 nm. The data for those reactions studied in the presence of residual oxygen are summarized in Tables 2 and 3.

The data in Table 2 for the reaction of $BQCN^+$ (0.5 mM) with MAH (40 mM) at 298 K in the presence of residual oxygen show very little variation in k_{app} during the early stages of the reaction but continuously increase as the first HL is approached. The other new information available from the data in Table 2 is the magnitude of SD of data from repetitive stopped-flow shots. In this case, the SD is on the order of 3–5% of the k_{app} values. The three data sets in Table 2 were obtained over a time period of about 6 months and were completely independent of one another, and the duplicate data sets for MAH result in significant differences in $KIE_{app}(1)$ and $KIE_{app}(2)$. The reason for this may be related to differences in residual oxygen concentrations.

In the presence of residual air the k_{app} obtained from the reactions of MAH/MAH-d_2 (0.5 mM) with $BQCN^+$ (40 mM) in AN were observed (Table 3) to be nearly independent of

dx.doi.org/10.1021/jo301874q | J. Org. Chem. 2012, 77, 9286–9297

Table 3. Changes in k_{app} and Standard Deviations (SD) as a Function of the Degree of Reaction Analyzed for the Reactions of MAH/MAH-d_2 (0.5 mM) with BQCN$^+$ (40 mM) in AN at 298 K in the Presence of Residual Oxygen at 430 nm

MAH[a]								
data set 1		data set 2		MAH-d_2[a]				
$10^4 \times k_{app}/s^{-1}$	$10^4 \times$ SD	$10^4 \times k_{app}/s^{-1}$	$10^4 \times$ SD	$10^4 \times k_{app}/s^{-1}$	$10^4 \times$ SD	$KIE_{app}(1)$	$KIE_{app}(2)$	segment
5.95	0.54	6.25	0.36	1.15	0.34	5.17	5.43	1
6.06	0.47	6.36	0.23	1.23	0.13	4.93	5.17	2
6.01	0.38	6.34	0.15	1.10	0.08	5.46	5.76	3
5.99	0.31	6.32	0.12	1.06	0.08	5.65	5.96	4
5.98	0.24	6.31	0.08	1.07	0.09	5.59	5.90	5
5.99	0.12	6.32	0.04	1.12	0.05	5.35	5.64	6
6.03	0.07	6.33	0.04	1.14	0.02	5.29	5.55	7
6.06	0.05	6.31	0.03	1.13	0.02	5.36	5.58	8
6.07	0.04	6.29	0.03	1.14	0.02	5.32	5.52	9
6.07	0.03	6.28	0.02	1.14	0.02	5.32	5.51	10
6.07	0.02	6.27	0.02	1.13	0.02	5.37	5.55	11
6.06	0.02	6.26	0.02	1.13	0.02	5.36	5.54	12
6.05	0.02	6.25	0.02	1.13	0.02	5.35	5.53	13
6.05	0.02	6.25	0.02	1.13	0.02	5.35	5.53	14
6.04	0.03	6.24	0.02	1.13	0.02	5.35	5.52	15
6.04	0.03	6.23	0.02	1.13	0.02	5.35	5.51	16
6.03	0.04	6.21	0.02	1.13	0.02	5.34	5.50	17
6.03	0.04	6.21	0.02	1.13	0.02	5.34	5.50	18
6.03	0.04	6.20	0.02	1.13	0.02	5.34	5.49	19
6.02	0.04	6.19	0.02	1.13	0.02	5.33	5.48	20
6.02	0.04	6.18	0.02	1.13	0.02	5.33	5.47	21
6.02	0.05	6.17	0.02	1.13	0.02	5.33	5.46	22
6.02	0.05	6.16	0.02	1.13	0.02	5.33	5.45	23
6.01	0.05	6.15	0.02	1.13	0.02	5.32	5.44	24

[a]Average of 10 stopped-flow repetitions.

Table 4. Apparent Rate Constants and Apparent Kinetic Isotope Effects at Short Times for the Reactions of MAH/MAH-d_2 (10 mM) with BQCN$^+$ (40 mM) in AN at 298 K in the Presence of Residual Oxygen at 440 nm (over the first 0.3% reaction)

	data set 1[a]			data set 2[a]			data set 3[a]			
time/s	$10^4 \times k_{app}^{H1}/s^{-1}$	$10^4 \times k_{app}^{D1}/s^{-1}$	KIE_{app}^{1}	$10^4 \times k_{app}^{H2}/s^{-1}$	$10^4 \times k_{app}^{D2}/s^{-1}$	KIE_{app}^{2}	$10^4 \times k_{app}^{H3}/s^{-1}$	$10^4 \times k_{app}^{D3}/s^{-1}$	KIE_{app}^{3}	segment
0.019	13.1	10.2	1.28	12.3	5.93	2.08	11.2	11.6	0.97	1
0.031	10.2	3.36	3.04	10.2	5.17	1.97	7.75	6.83	1.13	2
0.044	8.78	3.96	2.22	9.04	3.14	2.88	8.41	5.25	1.60	3
0.056	8.52	4.23	2.01	8.61	3.21	2.68	8.07	5.01	1.61	4
0.069	8.22	3.23	2.54	8.60	3.40	2.53	7.58	4.75	1.60	5
0.13	6.20	1.76	3.52	6.18	1.81	3.41	5.77	2.65	2.18	6
0.26	5.54	1.11	4.99	5.21	0.76	6.86	5.14	1.08	4.76	7
0.38	5.49	0.87	6.31	5.06	0.68	7.44	4.98	0.83	6.00	8
0.51	5.52	0.85	6.49	5.11	0.74	6.91	5.03	0.83	6.06	9
0.63	5.54	0.89	6.22	5.14	0.81	6.35	5.08	0.88	5.77	10
0.76	5.59	0.95	5.88	5.17	0.88	5.88	5.14	0.92	5.59	11
0.88	5.62	0.99	5.68	5.20	0.93	5.59	5.19	0.97	5.35	12
1.01	5.64	1.01	5.58	5.21	0.97	5.37	5.21	0.99	5.26	13
1.13	5.66	1.04	5.44	5.22	0.99	5.27	5.22	1.01	5.17	14
1.26	5.67	1.06	5.35	5.24	1.01	5.19	5.24	1.02	5.14	15
1.38	5.67	1.07	5.30	5.25	1.02	5.15	5.25	1.03	5.10	16
1.51	5.68	1.08	5.26	5.25	1.03	5.10	5.25	1.04	5.05	17
1.63	5.68	1.09	5.21	5.25	1.03	5.10	5.26	1.05	5.01	18
1.76	5.68	1.10	5.16	5.26	1.04	5.06	5.26	1.05	5.01	19
1.88	5.69	1.10	5.17	5.26	1.05	5.01	5.26	1.06	4.96	20
2.01	5.69	1.11	5.13	5.26	1.05	5.01	5.27	1.06	4.97	21
2.13	5.69	1.11	5.13	5.26	1.06	4.96	5.27	1.07	4.93	22
2.26	5.70	1.11	5.14	5.26	1.06	4.96	5.27	1.07	4.93	23
2.38	5.71	1.11	5.14	5.26	1.06	4.96	5.27	1.07	4.93	24

[a]Average of 20 stopped-flow repetitions.

dx.doi.org/10.1021/jo301874q | J. Org. Chem. 2012, 77, 9286−9297

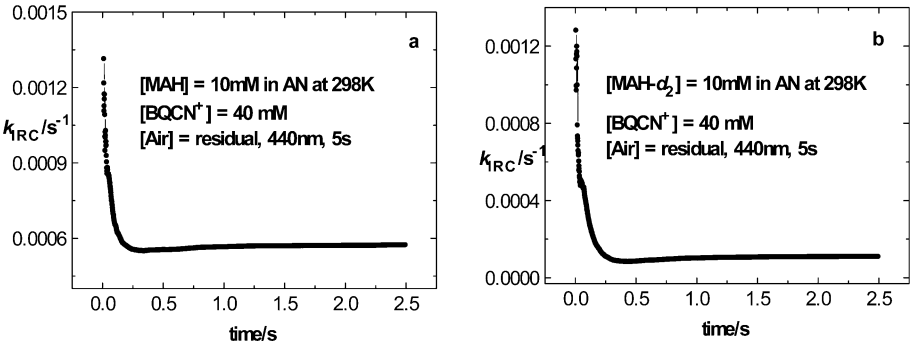

Figure 3. Apparent instantaneous rate constants (k_{IRC}) vs time plots for the reactions of $BQCN^+$ (40 mM) with MAH (a)/(MAH-d_2) (b) (10 mM) in AN containing residual air at 298 K at 440 nm.

Table 5. Changes in k_{app} and Standard Deviations (SD) as a Function of the Degree of Reaction Analyzed for the Reactions of MAH/MAH-d_2 (40 mM) with $BQCN^+$ (0.5 mM) in AN at 298 K Half-Saturated with Air at 430 nm

MAH[a]								
data set 1		data set 2		MAH-d_2[a]				
$10^4 \times k_{app}/s^{-1}$	$10^4 \times$ SD	$10^4 \times k_{app}/s^{-1}$	$10^4 \times$ SD	$10^4 \times k_{app}/s^{-1}$	$10^4 \times$ SD	$KIE_{app}(1)$	$KIE_{app}(2)$	segment
8.23	0.28	13.6	0.37	2.71	0.23	3.04	5.02	1
8.59	0.08	13.9	0.12	2.59	0.09	3.32	5.37	2
8.59	0.11	13.9	0.14	2.57	0.06	3.34	5.41	3
8.53	0.13	14.1	0.09	2.60	0.04	3.28	5.42	4
8.48	0.11	14.1	0.09	2.63	0.04	3.22	5.36	5
8.35	0.08	14.3	0.08	2.70	0.04	3.09	5.30	6
8.27	0.07	14.7	0.10	2.72	0.05	3.04	5.40	7
8.25	0.05	15.2	0.09	2.70	0.04	3.06	5.63	8
8.25	0.04	15.6	0.10	2.69	0.05	3.07	5.80	9
8.31	0.01	16.0	0.09	2.68	0.05	3.10	5.97	10
8.49	0.03	16.4	0.09	2.67	0.04	3.18	6.14	11
8.75	0.06	16.7	0.09	2.65	0.04	3.30	6.30	12
9.06	0.08	17.1	0.09	2.64	0.04	3.43	6.48	13
9.39	0.09	17.5	0.09	2.62	0.04	3.58	6.68	14
9.74	0.11	17.9	0.08	2.61	0.04	3.73	6.86	15
10.1	0.13	18.3	0.09	2.61	0.03	3.87	7.01	16
10.5	0.14	18.7	0.08	2.60	0.03	4.04	7.19	17
10.9	0.16	19.2	0.09	2.59	0.03	4.21	7.41	18
11.3	0.18	19.6	0.10	2.59	0.03	4.36	7.57	19
11.7	0.20	20.2	0.10	2.59	0.03	4.52	7.80	20
12.1	0.22	20.7	0.11	2.59	0.03	4.67	7.99	21
12.5	0.24	21.3	0.11	2.60	0.03	4.81	8.19	22
12.9	0.26	22.0	0.12	2.60	0.03	4.96	8.46	23
13.4	0.27	22.8	0.13	2.61	0.03	5.13	8.74	24

[a]Average of 10 stopped-flow repetitions.

segment number. Earlier[12] using lower [MAH/MAH-d_2] we found no deviations in reactions of MAH or MAH-d_2 over the first HL at temperatures lower than 308 K. The latter observation is confirmed by the data in Table 3. As before, the three data sets in Table 3 were collected over a several month period and the differences in the duplicate MAH data sets are reasonably small, as reflected by the values of $KIE_{app}(1)$ and $KIE_{app}(2)$.

Under these conditions, the [MA^+] which was monitored at 430 nm is very low at short times, so the concentration of the limiting reagents (MAH/MAH-d_2) was increased to 10 mM from 0.5 mM. This increase in [substrate] resulted in absorbance changes that could be monitored with a higher degree of accuracy. Although these conditions are not strictly pseudo-first-order, only the first 0.3% of the reaction was followed, which essentially eliminates significant error for this reason. The tabulated data for these experiments are shown in Table 4. The purpose of the three data sets was to derive KIE_{app} at short times. The three data sets were conducted independently of each other over a period of months. A comparison of the three KIE_{app} time profiles shows that they start at low values and end at steady-state values.

Instantaneous rate constant (IRC) analysis[26,29] of the reactions between MAH/MAH-d_2 and $BQCN^+$ in AN is illustrated by the plots in Figure 3. An important feature of the plots in Figure 3 is that the experimental data for these figures was the increase in absorbance at 440 nm. Neither the reactants nor the CT complex has large enough extinction coefficients at this wavelength to have significant absorbance at the low concentration of these species. In the absence of another

dx.doi.org/10.1021/jo301874q | J. Org. Chem. 2012, 77, 9286−9297

intermediate at this wavelength, the expected response for MA^+ evolution is a plot that approaches zero at very short times and evolves to the steady-state value with increasing times. Obviously, the latter is not the case and the decreasing values of k_{IRC} in both plots in Figure 3 correspond to the decrease in the concentration of an intermediate on the way toward the steady state. The same conclusion can be arrived at from the decreasing values of k_{app} and the increasing values of KIE_{app} in Table 4. The very low values of KIE_{app} at short times led to the same conclusion.

Reactions in the Presence of Intentionally Included Air. Data for reactions in AN half-saturated with air for reactions of $BQCN^+$ (0.5 mM) with MAH and MAH-d_2 (40 mM) at 298 K are summarized in Table 5. The apparent rate constants for the reaction of MAH vary considerably, from 0.000 823 in segment 1 to 0.001 34 s^{-1} in segment 24 (data set 1) and from 0.000 136 to 0.000 228 (data set 2). The increase in k_{app} with segment number can be attributed to a chain reaction initiated by oxygen in which oxygen intercepts an intermediate in the reaction, resulting in the increase in the rate of product formation. On the other hand, k_{app} for the MAH-d_2 reaction was essentially invariant within experimental error over all segments. The latter suggests that MAH-d_2 is, as expected, much less prone than MAH to react with O_2.

The values of k_{app} in Table 6 are for the reaction of MAH (0.5 mM) with $BQCN^+$ (40 mM) in AN half-saturated with air. The point of most interest is the fact that k_{app} in this case is only moderately changed in going from segment 1 to segment 24.

Table 6. Changes in k_{app} and Standard Deviations (SD) as a Function of the Degree of Reaction Analyzed for the Reaction of MAH (0.5 mM) with $BQCN^+$ (40 mM) in AN at 298 K Half-Saturated with Air at 430 nm[a]

time/s	$10^4 \times k_{app}/s^{-1}$	$10^4 \times$ SD	segment
2.47	6.20	0.21	1
4.72	6.20	0.17	2
6.97	6.30	0.17	3
9.22	6.33	0.13	4
11.5	6.34	0.13	5
22.7	6.26	0.07	6
45.2	6.11	0.01	7
67.7	6.03	0.02	8
90.2	6.00	0.03	9
112.7	5.97	0.04	10
135.2	5.95	0.04	11
157.7	5.93	0.03	12
180.2	5.92	0.03	13
202.7	5.91	0.03	14
225.2	5.90	0.03	15
247.7	5.88	0.03	16
270.2	5.87	0.03	17
292.7	5.86	0.03	18
315.2	5.85	0.02	19
337.7	5.84	0.02	20
360.2	5.83	0.02	21
382.7	5.82	0.02	22
405.2	5.80	0.02	23
427.7	5.79	0.01	24

[a]Average of 10 stopped-flow repetitions.

It should be noted that the SD at the top of the columns 2, 4, and 6 in Tables 2−6 are significant and decrease progressively to very small values. The reason for this trend is that SD values decrease directly in proportion to the increase in the number of points taken into the correlation.

Kinetic Isotope Effects for the Reaction of $BQCN^+$ with MAH in AN at 298 K at Short Times. The observation of time-dependent KIE has been shown to be a very effective tool in mechanism analysis.[28] It is particularly important to attempt to estimate the KIE as zero-time is approached, since an extrapolated KIE equal to 1 is very strong evidence that there is no C−H bond breaking in the first step of a multistep mechanism. The observed value of KIE_{app} at the shortest time (0.97) in Table 4 is certainly associated with great enough error to justify rounding off to 1.0. The time-dependence of KIE is only observed at times before steady state is reached. This implies that a plot of KIE_{app} vs time can be used to estimate the time necessary to reach steady state. Although the latter is correct, it should be pointed out that a much more accurate analysis can be carried out using plots of k_{app}^H and k_{app}^D. This allows for the fact that the time necessary for steady state to be reached may differ for the two different substrates.

The determination of the time necessary to reach steady state for the reactions of $BQCN^+$ (40 mM) with MAH/MAH-d_2 (10 mM) in AN at 298 K in the presence of residual air is illustrated in Figure 3. The time to reach steady state under these conditions can be estimated to be on the order of 0.5 s for both isotopic substrates [MAH (Figure 3a) and MAH-d_2 (Figure 3b)].

A fact that must be considered when analyzing data obtained at very low conversions is that absorbance due to products is very low under these conditions. As a consequence of this, parameters based on changes in product absorbance are subject to much greater uncertainty than those observed at higher conversions. This is demonstrated by a comparison of the data from three identical sets of experiments in Table 4. The first set of experiments resulted in KIE_{app} ranging from 1.28 to 5.14, in the second set from 2.08 to 4.96, and in the third set the values ranged from 0.97 to 4.93 (KIE_{app} vs time plots shown in Supporting Information, Figure S-2). The differences in the three ranges are almost entirely due to the large differences in the initial values. Under the reaction conditions that the data in Table 4 were gathered, the corresponding half-lives for the reaction of MAH were about 1000 s and that for MAH-d_2 was close to 5000 s.

The data for the reaction of MAH (10 mM) with $BQCN^+$ (0.5 mM) in AN in the presence of residual oxygen shown in Table 7 are for three identical sets of reactions over the first half-life. The data not only show relatively small SD values but also only small differences in the values of k_{app} over the entire range of segments. The reproducibility of the data for the three experiments under identical conditions is remarkable and consistent with that observed in other studies using the same methodology.[27,28]

The data in Table 8 for the isotopic substrates encompass conversion in the range from 0 to 0.6%. In connection with the point we are making concerning reliability of data depending upon the concentration of product [MA^+] analyzed is clearly illustrated by the columns labeled 10^4 SD. The SD values in the first row (segment 1) are on the order of 40% of the pertinent k_{app} values, while those in segment 24 are only 0.3% of the corresponding k_{app} values. The low value of KIE_{app} in segment 1

Table 7. Changes in k_{app} and Standard Deviations (SD) as a Function of the Degree of Reaction Analyzed for the Reaction of MAH (10 mM) with $BQCN^+$ (0.5 mM) in AN at 298 K in the Presence of Residual Oxygen at 450 nm over 1 HL

data set 1[a]		data set 2[a]		data set 3[a]		average		
$10^4 \times k_{app1}/s$	$10^4 \times$ SD	$10^4 \times k_{app1}/s$	$10^4 \times$ SD	$10^4 \times k_{app1}/s$	$10^4 \times$ SD	$10^4 \times k_{app1}/s$	±	segment
1.69	0.08	1.75	0.07	1.66	0.07	1.70	0.05	1
1.72	0.06	1.72	0.05	1.66	0.03	1.70	0.03	2
1.71	0.04	1.75	0.04	1.68	0.04	1.71	0.04	3
1.71	0.03	1.77	0.03	1.69	0.04	1.72	0.04	4
1.71	0.02	1.77	0.02	1.71	0.04	1.73	0.03	5
1.71	0.01	1.77	0.02	1.74	0.04	1.74	0.03	6
1.71	0.02	1.77	0.02	1.74	0.03	1.74	0.03	7
1.72	0.02	1.77	0.02	1.74	0.04	1.74	0.03	8
1.72	0.02	1.78	0.02	1.75	0.04	1.75	0.03	9
1.73	0.02	1.79	0.02	1.75	0.04	1.76	0.03	10
1.74	0.02	1.80	0.02	1.76	0.04	1.77	0.03	11
1.75	0.03	1.81	0.03	1.78	0.05	1.78	0.03	12
1.77	0.03	1.83	0.03	1.79	0.05	1.80	0.03	13
1.78	0.03	1.85	0.04	1.81	0.06	1.81	0.04	14
1.80	0.04	1.87	0.04	1.82	0.07	1.83	0.04	15
1.81	0.04	1.88	0.05	1.83	0.07	1.84	0.04	16
1.82	0.05	1.89	0.05	1.84	0.08	1.85	0.04	17
1.83	0.05	1.90	0.05	1.85	0.08	1.86	0.04	18
1.84	0.06	1.91	0.05	1.86	0.09	1.87	0.04	19
1.84	0.06	1.92	0.06	1.87	0.09	1.88	0.04	20
1.85	0.06	1.93	0.06	1.87	0.09	1.88	0.04	21
1.85	0.07	1.93	0.06	1.88	0.09	1.89	0.04	22
1.85	0.07	1.94	0.06	1.88	0.10	1.89	0.05	23
1.85	0.07	1.94	0.06	1.88	0.10	1.89	0.05	24

[a]Average of 10 stopped-flow repetitions.

Table 8. Changes in k_{app} and KIE_{app} as a Function of the Degree of Reaction (over the first 0.6% reaction) Analyzed for the Reactions of MAH/MAH-d_2 (10 mM) with $BQCN^+$ (40 mM) in AN at 298 K in the Presence of Residual Oxygen at 440 nm

	MAH[a]		MAH-d_2[a]			
time/s	$10^4 \times k_{app}^H$	$10^4 \times$ SD	$10^4 \times k_{app}^D$	$10^4 \times$ SD	KIE_{app}	segment
0.032	10.26	4.02	8.24	2.73	1.25	1
0.057	7.99	2.93	4.59	1.97	1.74	2
0.082	7.16	1.79	2.49	1.40	2.88	3
0.107	6.84	1.33	1.71	1.11	4.00	4
0.132	6.60	0.92	1.34	0.89	4.93	5
0.257	5.80	0.29	0.69	0.47	8.41	6
0.507	5.89	0.16	0.77	0.26	7.65	7
0.757	6.07	0.08	0.90	0.14	6.74	8
1.007	6.10	0.06	0.98	0.10	6.22	9
1.257	6.13	0.04	1.02	0.09	6.01	10
1.507	6.15	0.03	1.06	0.08	5.80	11
1.757	6.16	0.03	1.07	0.07	5.76	12
2.007	6.16	0.02	1.08	0.05	5.70	13
2.257	6.17	0.02	1.08	0.04	5.71	14
2.507	6.17	0.02	1.08	0.04	5.71	15
2.757	6.17	0.01	1.08	0.04	5.71	16
3.007	6.16	0.02	1.09	0.04	5.65	17
3.257	6.17	0.02	1.10	0.04	5.61	18
3.507	6.17	0.02	1.10	0.03	5.61	19
3.757	6.17	0.02	1.11	0.03	5.56	20
4.007	6.18	0.02	1.11	0.03	5.57	21
4.257	6.18	0.02	1.12	0.03	5.52	22
4.507	6.18	0.02	1.12	0.03	5.52	23
4.757	6.18	0.02	1.12	0.02	5.52	24

[a]Average of three sets of 20 stopped-flow repetitions.

surely is indicative that the latter approaches unity as reaction time approaches zero.

DISCUSSION

The conventional kinetic data in Table 1 suffice to answer the question regarding whether or not the reactions follow a one-step or a complex mechanism. Under all conditions studied—(a) $BQCN^+$ as limiting reagent in AN with residual oxygen, (b) $BQCN^+$ as limiting reagent in AN half-saturated with air, (c) MAH as limiting reagent in AN with residual oxygen, and (d) MAH as limiting reagent in AN half-saturated with air—the rate constants derived and the intercepts of linear correlation plots varied as the degree of reaction of the analyses increased. This leaves little room for doubt that the reaction between MAH and $BQCN^+$ in AN follows a multistep mechanism.

The successive correlation data in Table 2 (condition a) over about 1 HL show that even in the absence of intentionally added air at 298 K there are significant changes in k_{app} with time. The data also show that under these conditions there are differences in k_{app} in the two sets of experiments. These differences could be a consequence of differences in the trace oxygen concentration. We have pointed out that in another comparison of three identical runs (Table 7) the differences observed in k_{app} are very small.

The data in Table 5 are under condition b and once again we observe that the two different sets of k_{app}^H differ and give rise to two sets of KIE_{app} (using a single set of k_{app}^D) ranging from 3.04 to 5.13 for set 1 and from 5.02 to 8.74 for set 2. Although the values of KIE are different in the two sets, most likely due to differences in $[O_2]$, the trends in the two KIE_{app} sets are similar, beginning at short times at relatively low values and increasing by 69 and 74% over time for sets 1 and 2, respectively.

In the absence of intentionally added air with MAH as limiting reagent (condition c) the data are much more reproducible from one data set to the next. This is illustrated in Table 3. Under these conditions the variations in KIE_{app} are much smaller, settling down at about 5.33 for set 1 and 5.44 for set 2, respectively. The larger variations in values from segments 1−5 are consistent with the larger standard deviations observed for data in these segments.

The conditions for the reactions described by the data in Table 4 are quite different from those previously discussed. The concentration of the limiting reagents (MAH/MAH-d_2) was increased to 10 mM. The purpose of this was to allow the reactions to be analyzed with very low conversions (0.3%) and still produce high enough product concentrations so that the precision in the rate constants would not suffer too greatly. Standard deviations for the three data sets are appreciably larger than for the data discussed above, but the overall result, the time-dependent KIE_{app}, are reasonably close for the three data sets, again with the largest variations observed in the early reaction segments. The ranges of KIE_{app} were observed to be 1.28−5.14, 1.97−4.96, and 0.97−4.93 for data sets 1, 2, and 3,

dx.doi.org/10.1021/jo301874q | J. Org. Chem. 2012, 77, 9286−9297

Scheme 2. Proposed Multistep Mechanism for the Reaction of MAH with $BQCN^+$ in AN in the Presence of Residual or Intentionally Added Air at 298 K[a]

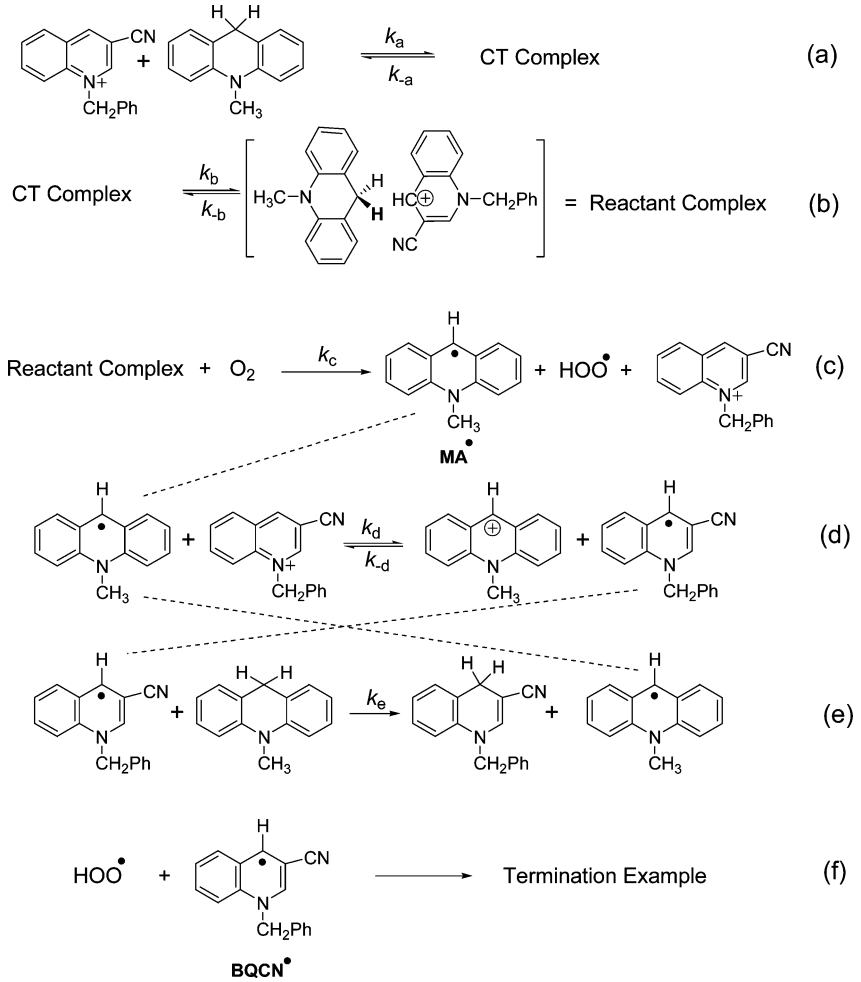

[a]The dashed lines connecting structures in steps d and e are between the propagating species in the two equations.

respectively, and the average value was 1.44 for the initial values.

The mechanistic significance of KIE_{app} approaching unity at near zero time is that it provides very strong evidence that there is no KIE in the first step of the reaction.[28] A further conclusion which can be arrived at from this observation, when product evolution is followed, is that hydride (or hydrogen atom or proton) transfer is not rate-determining under these circumstances. This would suggest that the mechanism of the reaction showing these kinetic characteristics must involve a minimum of three microscopic steps.

Data for another set of reactions under still different conditions, 10 mM MAH and 0.50 mM $BQCN^+$, are illustrated in Table 7. The data of most interest is in column 7, which shows that the average value of k_{app} changes smoothly from 1.70 to 1.89 over 1 HL with very small standard deviations. It is evident that under these conditions there is no problem with the precision of the measurements or the data, and that even in the presence of only residual concentrations of air, there is a definitive dependence of k_{app} on time.

This leads us once again to the dependence of KIE_{app} on the extent or time of reaction and to the data in Table 8. In this case, the limiting reagents are MAH and MAH-d_2 (10 mM) in the presence of $BQCN^+$ (40 mM). We observed that high precision of the data was achieved (Table 8) under these conditions during the first 0.6% of the reaction. At this low degree of conversion, the deviation from pseudo-first-order kinetics is expected to be minimal. The data in Table 8 strengthen our case that KIE_{app} for this reaction is time-dependent and approaches unity as the time approaches 0. In this case, KIE_{app} was observed to be equal to 1.25 at short times and to increase relatively rapidly to a maximum value of 8.41 and then slowly settle down to a value equal to 5.52 in the later segments of the reaction (Supporting Information, Figure S-2).

Before suggesting a mechanism that describes this massive amount of experimental data, it is helpful to summarize the mechanistic evidence. The most pertinent evidence is summarized below. The first point is very important and seems difficult to argue with.

(1) The conventional pseudo-first-order kinetics are inconsistent with a one-step mechanism.[32]
(2) The rate of the reaction is dependent upon $[O_2]$, and the increase in k_{app} with time is even observed in the presence of only residual air in a glovebox under a nitrogen atmosphere.
(3) KIE_{app} values under a variety of conditions approach 1.0 at short times before proceeding to a maximum value and then slowly decreasing.

dx.doi.org/10.1021/jo301874q | J. Org. Chem. 2012, 77, 9286–9297

(4) The air effect is much more prominent when [MAH] is in large excess.

The observation of the air effect requires that O_2 reacts with some species, either reactant or intermediate. The obvious possibility is that O_2 abstracts a hydrogen atom from the 10-position of MAH. This reaction apparently takes place but at a very low rate (Supporting Information, Figures S-3 and S-4) in the absence of $BQCN^+$ in AN. It appears that the H atoms at the 10-position of MAH require activation to make the H-atom abstraction reaction feasible at rates high enough to be significant in the product-forming reaction of MAH with $BQCN^+$. However, it is likely that the reaction does provide enough radicals to serve as an initiator in a chain process.

Finally, the approach of KIE_{app} toward unity as the time approaches zero suggests not only that there is no KIE in the first step of the reaction but also that the mechanism involves a minimum of three microscopic reactions. We believe that the chain mechanism illustrated in Scheme 2 takes into account all of the experimental data and the points listed above. The reaction between MAH and oxygen is not included in the scheme but must be considered to be an initiation step.

We will begin the mechanism discussion by justifying each step in Scheme 2. In our previous investigation, we found that the CT complex formed (step a) at a rate too rapid to be follow by stopped-flow with an equilibrium constant close to 1.0 at 298 K.[12] The CT complex could be the intermediate reacting with oxygen. However, we do not believe that the loosely bound CT complex would change the reactivity of MAH sufficiently to enhance the rate of H-atom transfer to O_2 to the degree necessary for this reaction to take part in this mechanism. We view the formation of the "reactant complex" (step b) to involve the extrusion of solvent between the two entities in the CT complex and movement of atoms in the latter to an arrangement more conducive to the bond changes that must take place in going to the transition state for hydrogen atom (or hydride in mechanism 1) transfer (step b). We propose that the three-dimensional structure of the reactant complex is similar to that of the CT complex but tighter. Once MAH radical is formed (step c), the chain mechanism (steps d and e) takes place. The dashed lines in Scheme 2 connect chain carriers in the two steps (d and e). The product formation step (step 3 in Scheme 1) of the polar mechanism takes place concurrently with the chain mechanism and under some conditions is expected to dominate, i.e., when the substrate is MAH-d_2 and when the limiting reagent is MAH. The radical reactions (steps d and e) are expected to take place very rapidly. During the pre-steady-state period of the overall reaction, steps a and b dominate, and at times approaching zero, the mechanism predicts that KIE_{app} will approach unity, as was observed experimentally.

Before concluding we would like to return to Perrin's[13] apparently logical argument that the rate constant (k_b) that we reported[12] in mechanism 1 is too small for the dissociation of a weakly bound complex. The complex referred to was the CT complex, for which the equilibrium constant was reported to be close to 1.0.[12] We realized that the CT complex could not be the species responsible for the deviations from first-order kinetics and proposed another intermediate, which we called the reactant complex, which most likely forms from the CT complex. We do not know the structure of the reactant complex and therefore cannot use quantitative terms in describing its properties, in particular the Gibb's free energy of conversion to the CT complex, not dissociation. But what we have argued before[12] and still believe is that the reactant complex is tight by the virtue of the structural and solvation changes that must take place to form from the CT complex. The latter process may have a significant entropic contribution, especially if solvation changes lag behind bond changes, as is often proposed. A fact that must always be kept in mind when proposing a mechanism is that it must be consistent with the experimental evidence. The mechanism is then generally accepted as correct until new experimental data rule it out.

A logical question to ask is, why did we not observe deviations from simple mechanism kinetics at temperatures below 308 K in our 2003 study? The fact that we used a very limited range of extent of reaction (0.05−0.50) in the earlier study is the main factor for the latter but not the only one. Another factor contributing to that observation is that oxygen participation is much more prevalent when MAH is the reactant in excess, conditions that were not examined in our earlier study.[12] The final factor is that our new kinetic methodology, based upon the traditional first-order analysis, that involves multiscan stopped-flow spectrophotometry allows us to detect much smaller deviations from simple mechanism behavior than the conventional UV−vis spectrophotometry used in our 2003 study. Also, it should be pointed out that the reproducibility in measurements when MAH is in large excess is substantially lower than when $BQCN^+$ is the reactant in large excess.

Facts about Mechanism 1 and the Importance of the Ratio, k_b/k_p. The apparent rate constant according to mechanism 1, $k_{app} = k_p k_f/(k_p + k_b)$, can be rewritten as

$$k_{app} = \frac{k_f}{1 + k_b/k_p} \tag{4}$$

to emphasize the importance of k_b/k_p in the kinetic response to the mechanism. The experimental value of the k_{app} at 299 K, where MAH (1.5 mM) is allowed to react with BQCN (9 mM), is on the order of 0.017 M^{-1} s^{-1} and the value of K_{CT} reported in 2003 is equal to 1 M^{-1}.[12] The data in Table 2 of that paper for k_p, k_f, and k_b are not experimental values but rather were estimated from the best fit data in the temperature range from 308 to 325 K. This was accomplished with aid of k_{app} at 299 K and extrapolation of the Arrhenius plot of the best fit data for k_p.

Perrin's[13] main criticism of our mechanism is related to our estimation of k_b equal to only 0.004 s^{-1} at 299 K (for example). He states that k_b has to be very much larger than we report. We do not have any argument with that statement. What we argue is that there is no basis for the general conclusion that all of our experimental data are erroneous and that we are chasing artifacts.[14−26] Although we no longer think the best fit rate constants[12] are applicable, since this work shows that the mechanism is much more complex than believed in 2003, we can now show that our best fit rate constants are not unique and that there are an infinite number of values of k_b that fit the data, depending upon the value of k_b/k_p. This is shown by the results of simple calculations, where k_f is held constant at 0.019 M^{-1} s^{-1} while k_b and k_p are varied systematically while k_b/k_p is kept constant. The value reported for k_{app} was 0.0165 M^{-1} s^{-1}.[12]

We see from the data in Table 9 that k_{app} remains constant while k_b is varied smoothly from 10^9 to 10^4 s^{-1}. The

dx.doi.org/10.1021/jo301874q | J. Org. Chem. 2012, 77, 9286−9297

Table 9. Magnitude of k_b in Best Fit Data is Variable Depending on k_b/k_p

$k_f/M^{-1}\ s^{-1}$	$k_p/M^{-1}\ s^{-1}$	k_b/s^{-1}	$1 + k_b/k_p$	$k_{app}/M^{-1}\ s^{-1}$
0.019	10^9	0.15×10^9	1.15	0.0165
0.019	10^8	0.15×10^8	1.15	0.0165
0.019	10^7	0.15×10^7	1.15	0.0165
0.019	10^6	0.15×10^6	1.15	0.0165
0.019	10^5	0.15×10^5	1.15	0.0165
0.019	10^4	0.15×10^4	1.15	0.0165

experimental data in our 2003 paper could have been fit with any of the lines of parameters in Table 9.

Another important aspect of the k_b/k_p ratio is how the latter is reflected in KIE_{app}. This ratio must be in the range from 0.01 to 100 in order to have any observable effect on KIE_{app}. The closer to a value of 1 for this ratio, the larger the effect on KIE_{app} will be. Outside of this range, the reaction mechanism will be indistinguishable from that for the simple one-step reaction. This fact can also be deduced from the denominator of eq 4.

CONCLUSIONS

The most important conclusion for the "big picture" is that the reaction of MAH with $BQCN^+$ in AN takes place by a multistep mechanism. Another conclusion of some general importance is that oxygen takes part in a chain process during this reaction and is important even under conditions where rigorous attempts are made to eliminate it by thorough degassing of the solutions before placing them in a glovebox containing the stopped-flow instrument under an atmosphere of purified nitrogen. This leads to the conclusion that the chain pathway of formal hydride transfer in biological systems in nature may also involve the participation of oxygen.

Another important conclusion of this work as well as of our other recent publications[27,28] is that these studies verify the value of the kinetic methods developed in our laboratory over the past 15 years, and they continue to be developed.

EXPERIMENTAL SECTION

Materials. *N*-Methylacridinium iodide was prepared from acridine (Aldrich) and a 3-fold excess of methyl iodide in a minimum amount of acetone. 10-Methyl-9,10-dihydroacridine was prepared by reduction of *N*-methylacridinium iodide using sodium borohydride in dry methanol, followed by recrystallization from absolute ethanol.[33] 10-Methyl-9,10-dihydroacridine 9,9-d_2 was prepared as described in the literature.[34] 1-Benzyl-3-cyanoquinolinium perchlorate was prepared by ion exchange of 1-benzyl-3-cyanoquinolinium bromide obtained from the reaction of 3-cyanoquinoline with benzyl bromide.[35] The bromide salt was dissolved in dry acetonitrile in the presence of a 50-fold excess of sodium perchlorate. After evaporation of the solvent, the residue was washed with water and collected by filtration. The process was repeated twice to ensure complete exchange. The resulting solid was recrystallized from absolute ethanol to give the perchlorate salt. ^1H NMR (300 MHz, CD_3CN): δ 6.18 (2H, s), 7.43 (5H, m), 8.10 (1H, m), 8.32 (1H, m), 8.44 (2H, d), 9.50 (1H, s), 9.55 (1H, s). Acetonitrile was refluxed and distilled over P_2O_5 under a nitrogen atmosphere and passed through an Al_2O_3 column before being taking into the glovebox.

Kinetic Experiments. Kinetic experiments were carried out using a Hi-Tech SF-61 DX2 stopped-flow spectrophotometer installed in a glovebox and kept under a nitrogen atmosphere. The temperature was controlled at 298 K using a constant temperature flow system connected directly to the reaction cell through a bath situated outside of the glovebox. All stopped-flow experiments included recording 10 absorbance−time profiles at 430 or 450 nm. Each experiment was repeated at least three times. The 2000-point absorbance−time curve data were collected over either more than 1 HL or more than 4 HL.

Absorbance−time (Abs−t) profiles for product evolution were analyzed individually by two different procedures. The first step in both procedures was to convert the Abs−t profiles to (1 − ER)−time profiles. This was carried out by dividing each absorbance value by the infinity value obtained from the product extinction coefficient and the reactant concentration and subtracting the value from 1.0. This procedure gave (1 − ER)−time profiles that decayed from (1 − ER) = 1 for either 1 or 4 HL, depending on which analysis procedure was used. For pseudo-first-order kinetic analysis, the (1 − ER)−time profiles were converted to −ln(1 − ER)−time profiles. For further processing, the individual 4 HL (1 − ER)−time profiles were first averaged to give the average profiles. The first kinetic procedure used was simply a least-squares linear correlation of the −ln(1 − ER)−time profiles to give the apparent pseudo-first-order rate constants over either 1, 2, 3, or 4 HL. The second procedure involved recording the Abs−t profiles over slightly more than the first HL followed by the sequential 24 linear correlations described in the Results section.

ASSOCIATED CONTENT

Supporting Information

Figures of kinetic data under various conditions. This material is available free of charge via the Internet at http://pubs.acs.org.

AUTHOR INFORMATION

Corresponding Author

*E-mail: vernon.parker@usu.edu

Notes

The authors declare no competing financial interest.

ACKNOWLEDGMENTS

This work was supported by a grant (ARRA: CHE-0923654) from the National Science Foundation. This support is gratefully acknowledged.

REFERENCES

(1) Kim, Y.; Truhlar, D. G.; Kreevoy, M. M. *J. Am. Chem. Soc.* **1991**, *113*, 7837.
(2) Kotchevar, A. T.; Kreevoy, M. M. *J. Phys. Chem.* **1991**, *95*, 10345.
(3) Kreevoy, M. M.; Kotchevar, A. T. *J. Am. Chem. Soc.* **1990**, *112*, 3579.
(4) Kreevoy, M. M.; Ostovic, D.; Lee, I. -S. H.; Binder, D. A.; King, G. W. *J. Am. Chem. Soc.* **1988**, *110*, 524.
(5) Ostovic, D.; Lee, I.-S. H.; Roberts, R. M. G.; Kreevoy, M. M. *J. Org. Chem.* **1985**, *50*, 4206.
(6) Kreevoy, M. M.; Lee, I.-S. H. *J. Am. Chem. Soc.* **1984**, *106*, 2550.
(7) Anne, A. J.; Moiroux, J.; Saveänt, J.-M. *J. Org. Chem.* **2000**, *65*, 7213.
(8) Schowen, R. L. Model Studies of Hydrogen Transfer Reactions (Chapter 4). In *Hydrogen-Transfer Reactions*; Hynes, J. T., Klinman, J. P., Limbach, H.-H., Schowen, R. L., Eds.; Wiley-VCH Verlag GMbH & Co.: Weinheim, Germany, 2007.
(9) Cheng, J.-P; Lu, Y.; Zhu, X.-Q.; Mu, L. *J. Org. Chem.* **1998**, *63*, 6108.
(10) Cheng, J.-P; Lu, Y. *J. Phys. Org. Chem.* **1997**, *10*, 577.
(11) Zhu, X.-Q.; Zhang, J.-Y.; Cheng, J.-P. *J. Org. Chem.* **2006**, *71*, 7007.
(12) Lu, Y.; Zhao, Y.; Handoo, K. L.; Parker, V. D. *Org. Biomol. Chem.* **2003**, *1*, 173.
(13) Perrin, C. L.; Zhao, C. *Org. Biomol. Chem.* **2008**, *6*, 3349.
(14) Parker, V. D.; Zhao, Y.; Lu, Y.; Zheng, G. *J. Am. Chem. Soc.* **1998**, *120*, 12720.
(15) Lu, Y.; Handoo, K. L.; Parker, V. D. *Org. Biomol. Chem.* **2003**, *1*, 36.
(16) Parker, V. D.; Lu., Y. *Org. Biomol. Chem.* **2003**, *1*, 2621.

(17) Lu, Y.; Zhao, Y.; Parker, V. D. *J. Am. Chem. Soc.* **2001**, *123*, 5900.
(18) Zhao, Y.; Lu, Y.; Parker, V. D. *J. Chem. Soc., Perkin Trans. 2* **2001**, 1481.
(19) Parker, V. D.; Zhao, Y. *J. Phys. Org. Chem.* **2001**, *14*, 604.
(20) Zhao, Y.; Lu, Y.; Parker, V. D. *J. Am. Chem. Soc.* **2001**, *123*, 1579.
(21) Handoo, K. L.; Lu, Y.; Zhao, Y.; Parker, V. D. *Org. Biomol. Chem.* **2003**, *1*, 24.
(22) Handoo, K. L.; Lu, Y.; Zhao, Y.; Parker, V. D. *J. Am. Chem. Soc.* **2003**, *125*, 9381.
(23) Parker, V. D.; Lu, Y.; Zhao, Y. *J. Org. Chem.* **2005**, *70*, 1350.
(24) Parker, V. D. *Pure Appl. Chem.* **2005**, *77*, 1823.
(25) Parker, V. D. *J. Phys. Org. Chem.* **2006**, *19*, 714.
(26) Hao, W.; Parker, V. D. *J. Org. Chem.* **2008**, *73*, 48.
(27) Parker, V. D.; Li, Z.; Handoo, K. L.; Hao, W.; Cheng, J.-P. *J. Org. Chem.* **2011**, *76*, 1250.
(28) Li, Z.; Cheng, J.-P.; Parker, V. D. *Org. Biomol. Chem.* **2011**, *9*, 4563.
(29) Parker, V. D.; Hao, W.; Li, Z.; Scow, R. *Int. J. Chem. Kinet.* **2012**, *44*, 2−12.
(30) Fukuzumi, S.; Ohkubo, K.; Tokuda, Y.; Suenubo, T. *J. Am. Chem. Soc.* **2000**, *122*, 4286.
(31) Achord, J. M.; Hussey, C. L. *Anal. Chem.* **1980**, *52*, 601.
(32) It could be argued that there is a one-step hydride transfer (obeying pseudo-first-order kinetics) accompanied by a radical chain mechanism to give the deviations from the pseudo-first-order rate law. However, the k_{app}−time plots in Figure 3 reveal that the reaction kinetics become complex at times too short for the chain mechanism to contribute to the kinetic response.
(33) Colter, A. K.; Charles, G. L.; Williamson, T. W.; Berry, R. E. *Can. J. Chem.* **1983**, *61*, 2544.
(34) Karrer, P.; Szabo, L.; Krishan, H. J. V.; Schwyzer, R. *Helv. Chem. Acta.* **1950**, *33*, 294.
(35) Roberts, R. M. G.; Ostovic, D.; Kreevoy, M. M. *J. Org. Chem.* **1983**, *48*, 2053.